CISM International Centre for Mechanical Sciences 582
Courses and Lectures

Peter Lugner *Editor*

Vehicle Dynamics of Modern Passenger Cars

International Centre for Mechanical Sciences

Springer

CISM International Centre for Mechanical Sciences

Courses and Lectures

Volume 582

The series presents lecture notes, monographs, edited works and proceedings in the field of Mechanics, Engineering, Computer Science and Applied Mathematics. Purpose of the series is to make known in the international scientific and technical community results obtained in some of the activities organized by CISM, the International Centre for Mechanical Sciences.

More information about this series at http://www.springer.com/series/76

Peter Lugner
Editor

Vehicle Dynamics of Modern Passenger Cars

Springer

Editor
Peter Lugner
Institute of Mechanics and Mechatronics
TU Wien
Vienna
Austria

ISSN 0254-1971 ISSN 2309-3706 (electronic)
CISM International Centre for Mechanical Sciences
ISBN 978-3-319-79007-7 ISBN 978-3-319-79008-4 (eBook)
https://doi.org/10.1007/978-3-319-79008-4

Library of Congress Control Number: 2018937684

Printed on acid-free paper

This Springer imprint is published by the registered company Springer International Publishing AG part of Springer Nature
The registered company address is: Gewerbestrasse 11, 6330 Cham, Switzerland

Preface

At the CISM course "Vehicle Dynamics of Modern Passenger Cars", a team of six international distinguished scientists presented advances regarding theoretical investigations of the passenger car dynamics and their consequences with respect to applications.

Today, the development of a new car and essential components and improvements are based strongly on the possibility to apply simulation programmes for the evaluation of the dynamics of the vehicle. This accelerates and shortens the development process. Therefore, it is necessary not only to develop mechanical models of the car and its components, but also to validate mathematical–mechanical descriptions of many special and challenging components such as e.g. the tire. To improve handling behaviour and driving safety, control schemes are integrated, leading to such properties as avoiding wheel locking or torque vectoring and more. Future developments of control systems are directed towards automatic driving to relieve and ultimately replace most of the mundane driving activities.

As a consequence, this book and its six sections—based on the lectures of the mentioned CISM course—aim to provide the essential features necessary to understand and apply the mathematic–mechanical descriptions and tools for the simulation of vehicle dynamics and its control. An introduction to passenger car modelling of different complexities provides basics for the dynamical behaviour and presents the vehicle models later used for the application of control strategies. The presented modelling of the tire behaviour, also for transient changes of the contact patch properties, provides the needed mathematical description. The introduction to different control strategies for cars and their extensions to complex applications using, e.g., state and parameter observers is a main part of the course. Finally, the formulation of proper multibody code for the simulation leads to the integration of individual parts. Examples of simulations and corresponding validations will show the benefit of such a theoretical approach for the investigation of the dynamics of passenger cars.

As a start, the first Chapter "Basics of Vehicle Dynamics, Vehicle Models" comprises an introduction to vehicle modelling and models of increasing complexity. By using simple linear models, the characteristics of the plane vehicle

motion (including rear wheel steering), driving and braking and the vertical motion are introduced. Models that are more complex show the influence of internal vehicle structures and effects of system nonlinearities and tire–road contact. Near Reality Vehicle Models, an assembly of detailed submodels, may integrate simple models for control tasks.

Chapter "Tire Characteristics and Modeling" first presents steady-state tire forces and moments, corresponding input quantities and results obtained from tire testing and possibilities to formulate tire models. As an example, the basic physical brush tire model is presented. The empirical tire model known as Magic Formula, a worldwide used tire model, provides a complex 3D force transfer formulation for the tire–road contact. In order to account for the tire dynamics, relaxation effects are discussed and two applications illustrate the necessity to include them.

Chapter "Optimal Vehicle Suspensions: A System-Level Study of Potential Benefits and Limitations" starts with fundamental ride and handling aspects of active and semi-active suspensions presented in a systematic way, starting with simple vehicle models as basic building blocks. Optimal, mostly linear-quadratic (H2) principles are used to gradually explore key system characteristics, where each additional model DOF brings new insight into potential benefits and limitations. This chapter concludes with practical implications and examples including some that go beyond the traditional ride and handling benefits.

Chapter "Active Control of Vehicle Handling Dynamics" starts with the principles of vehicle dynamics control: necessary basics of control, kinematics and dynamics of road vehicles starting with simple models, straight-line stability. The effects of body roll and important suspension-related mechanics (including the Milliken Moment Method) are presented. Control methods describing steering control (driver models), antilock braking and electronic stability control, all essential information for an improvement for the vehicle handling, are provided.

In Chapter "Advanced Chassis Control and Automated Driving", it is stated first that recently various preventive safety systems have been developed and applied in modern passenger cars, such as electronic stability system (ESS) or autonomous emergency braking (AEB). This chapter describes the theoretical design of active rear steering (ARS), active front steering (AFS) and direct yaw moment control (DYC) systems for enhancing vehicle handling dynamics and stability. In addition to recently deployed preventive safety systems, adaptive cruise control (ACC) and lane-keeping control systems have been investigated and developed among universities and companies as key technologies for automated driving systems. Consequently, fundamental theories, principles and applications are presented.

Chapter "Multibody Systems and Simulation Techniques" starts with a general introduction to multibody systems (MBS). It presents the elements of MBS and discusses different modelling aspects. Then, several methods to generate the equations of motion are presented. Solvers for ordinary differential equation (ODE) as well as differential algebraic equation (DAE) are discussed. Finally, techniques for "online" and "offline" simulations required for vehicle development including real-time applications are presented. Selected examples show the connection between simulation and test results.

The application of vehicle and tire modelling, the application of control strategies and the simulation of the complex combined system open the door to investigate a large variety of configurations and to select the desired one for the next passenger car generation. Only conclusive vehicle tests are necessary to validate and verify the simulation quality—an advantage that is utilized for modern car developments.

To summarize these aspects and methods, this book intends to demonstrate how to investigate the dynamics of modern passenger cars and the impact and consequences of theory and simulation for the future advances and improvements of vehicle mobility and comfort. The chapters of this book are generally structured in such a way that they first present a fundamental introduction for the later investigated complex systems. In this way, this book provides a helpful support for interested starters as well as scientists in academia and engineers and researchers in car companies, including both OEM and system/component suppliers.

I would like to thank all my colleagues for their great efforts and dedication to share their knowledge, and their engagement in the CISM lectures and the contributions to this book.

Vienna, Austria Peter Lugner

Contents

Basics of Vehicle Dynamics, Vehicle Models

Peter Lugner and Johannes Edelmann

Abstract For the understanding and knowledge of the dynamic behaviour of passenger cars it is essential to use simple mechanical models as a first step. With such kind of models overall characteristic properties of the vehicle motion can be investigated. For cornering, a planar two-wheel model helps to explain understeer–oversteer, stability and steering response, and influences of an additional rear wheel steering. Another planar model is introduced for investigating straight ahead acceleration and braking. To study ride comfort, a third planar model is introduced. Consequently, in these basic models, lateral, vertical and longitudinal dynamics are separated. To gain insight into e.g. tyre–road contact or coupled car body heave, pitch and roll motion, a 3D-model needs to be introduced, taking into account nonlinearities. Especially the nonlinear approximation of the tyre forces allows an evaluation of the four tyre–road contact conditions separately—shown by a simulation of a braking during cornering manoeuvre. A near reality vehicle model (NRVM) comprises a detailed 3D description of the vehicle and its parts, e.g. the tyres and suspensions for analysing ride properties on an arbitrary road surface. The vehicle model itself is a composition of its components, described by detailed sub-models. For the simulation of the vehicle motion, a multi-body-system (MBS)-software is necessary. The shown fundamental structure of the equations of motion allows to connect system parts by kinematic restrictions as well, using closed loop formulations. A NRVM also offers the possibility for approving a theoretical layout of control systems, generally by using one of the simple vehicle models as observer and/or part of the system. An example demonstrates the possibility of additional steering and/or yaw moment control by differential braking.

Keywords Vehicle dynamics · Vehicle handling · Basic models
Non-linear models

P. Lugner (✉) · J. Edelmann
Institute of Mechanics and Mechatronics, TU Wien, Vienna, Austria
e-mail: peter.lugner@tuwien.ac.at

P. Lugner (ed.), *Vehicle Dynamics of Modern Passenger Cars*,
CISM International Centre for Mechanical Sciences 582,
https://doi.org/10.1007/978-3-319-79008-4_1

1 Introduction

Important features of modern passenger cars with respect to vehicle dynamics are easy handling for normal driving, appropriate ride comfort, and support of the driver by control systems e.g. for lane keeping or in critical situations.

In addition to investigate the fundamental dynamic behaviour of the vehicle, theoretical methods support the engineer in an early stage of vehicle development in order to define basic vehicle layout properties, where no experiments are available, and also for understanding detailed dynamic properties of (sub) systems. Thereby the use of models of different complexity comprises the understanding of basic properties as well as the interaction with (human) control systems, by applying simulations with multi-body-system (MBS) programs, see Lugner (2007), Rill (2012). With the obtained results, the overall characteristics of the car can be interpreted and recommendations for details of components can be given, as well as the potential for future developments and improvements demonstrated.

Which kind of mathematical–dynamical vehicle model is needed/will be used is obviously a matter of the demanded degree of detail with respect to the investigated ride/handling quality. For the understanding and characterization of the basic behaviour with respect to the longitudinal and lateral dynamics and vertical motion, different linearized models may be used, see e.g. Mitschke and Wallentowitz (2014), Plöchl et al. (2015).

More complex models, including proper nonlinear descriptions of the tyre behaviour, are necessary to describe the spacial carbody motion and tyre–road contact to consider higher accelerations.

For the layout of vehicle components and their kinematic and dynamic interaction, detailed MBS-models including full nonlinearities are used to establish a near reality vehicle model (NRVM). Such a model also provides the possibility to investigate the behaviour of control systems in a theoretical environment—a necessity for the tuning of structures and parameters for a later realisation.

2 Simple (linear) Vehicle Models

By using basic (planar) linear models with a low number of degrees of freedom (DoF), the equation of motions may decouple with regard to lateral, longitudinal and vertical vehicle motion. Thus, cornering, longitudinal dynamics and vertical dynamics can be investigated independently.

2.1 Cornering, x-y-plane Motion

This well known simplified model of the vehicle is based on merging both wheels of an axle to a substitutive wheel (axle characteristics) in the centre of this axle, see Fig. 1. Furthermore, it is assumed that the whole model—called two-wheel model (or bicycle model)—may move in the x-y-plane only. Since the model is planar, the CG will also move in this plane only, e.g. Plöchl et al. (2015), Plöchl et al. (2014), Abe (2009), Popp and Schiehlen (2010). For the nomenclature and explanation of state variables see also DIN ISO 8855 (2013).

The relevant DoF for this model are the longitudinal and lateral motion and the rotation about a vertical axis, represented by the velocities v_x and v_y (or v and side slip angle of the vehicle β), and yaw rate $\dot{\psi} = r$, see Fig. 1.

With front and rear steering angles δ_F and δ_R as inputs to the vehicle, the kinematic description of the motion of the car provides the side slip angles of front and rear substitutive wheels with

$$\begin{aligned} \alpha_F &= \delta_F - \frac{v_y + l_F\dot{\psi}}{v_x} \\ \alpha_R &= \delta_R - \frac{v_y - l_R\dot{\psi}}{v_x} \end{aligned} \tag{1}$$

Fig. 1 Planar vehicle model

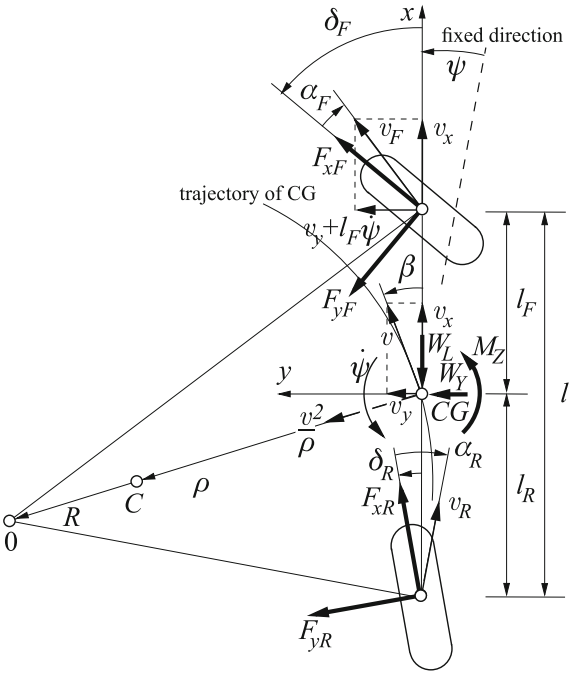

A linear model as basic description of the lateral tyre/axle forces

$$F_{yi} = C_i \alpha_i \qquad i = R, F \tag{2}$$

is applied, where the cornering stiffness C_i comprises properties of the tyres and the suspension stiffnesses.

With the aerodynamic forces W_L, W_Y and the aerodynamic moment M_Z the equations of motion are

$$x: \quad m(\dot{v} - a_q \beta) = \left(F_{xF} - F_{yF}\delta_F\right) + \left(F_{xR} - F_{yR}\delta_R\right) - W_L \tag{3}$$

$$y: \quad m(a_q + \beta \dot{v}) = \left(F_{xF}\delta_F + F_{yF}\right) + \left(F_{xR}\delta_R + F_{yR}\right) + W_Y \tag{4}$$

$$z: \quad I_Z \ddot{\psi} = \left(F_{xF}\delta_F + F_{yF}\right) l_F - \left(F_{xR}\delta_R + F_{yR}\right) l_R + M_Z \tag{5}$$

The lateral acceleration can be expressed by using the radius ρ of the curvature of the path of the *CG*

$$a_q = \frac{v^2}{\rho} \tag{6}$$

Considering the steering angles δ_F, δ_R and the longitudinal tyre/axle forces F_{xF}, F_{xR} (provided by the drive train and brake system) as input quantities, Eqs. (1)–(5), will describe the motion of the car by $v(t)$, $\psi(t)$, $\rho(t)$.

With the restriction of the linear description of the lateral tyre forces, neglecting the influence of the longitudinal force transfer and assuming small accelerations $\dot{v}$ or steady state conditions, Eqs. (4) and (5) are sufficient to describe the in-plane-motion of the vehicle.

For basic investigations of the cornering behaviour a constant longitudinal velocity is considered, leading to

$$v \cong v_x = \text{konst} \quad ; \quad v = (\dot{\beta} + \dot{\psi})\rho \tag{7}$$

$$a_q \cong a_y = v(\dot{\beta} + \dot{\psi}) \tag{8}$$

Moreover, for constant velocity v the longitudinal tyre forces will be small. Thus the expressions $F_{xi}\delta_i$ in (4) and (5) can be neglected. and the linear matrix equation of the linear two-wheel model is derived by

$$\dot{x} = \mathbf{F}x + \mathbf{G}\delta \tag{9}$$

$$x = \begin{bmatrix} v_y \\ \dot{\psi} \end{bmatrix} = \begin{bmatrix} v_y \\ r \end{bmatrix}, \quad \delta = \begin{bmatrix} \delta_F \\ \delta_R \end{bmatrix},$$

$$\mathbf{F} = \begin{bmatrix} -\frac{C_F+C_R}{mv_x} & -\frac{(l_F C_F - l_R C_R)}{mv_x} - v_x \\ -\frac{(l_F C_F - l_R C_R)}{I_Z v_x} & -\frac{l_F^2 C_F + l_R^2 C_R}{I_Z v_x} \end{bmatrix}, \quad \mathbf{G} = \begin{bmatrix} \frac{C_F}{m} & \frac{C_R}{m} \\ \frac{l_F C_F}{I_Z} & -\frac{l_R C_R}{I_Z} \end{bmatrix}$$

Another way to describe the system is to transfer (9) into a second-order-system, Kortüm and Lugner (1994)

$$\ddot{\beta} + 2K_1\dot{\beta} + K_2\beta = \frac{C_F}{mv_x}\dot{\delta}_F - \frac{C_F(l_F m v_x^2 - C_R l_R l)}{I_Z m v_x^2}\delta_F + \frac{C_R}{mv_x}\dot{\delta}_R - \frac{C_R(-l_R m v_x^2 - C_F l_F l)}{I_Z m v_x^2}\delta_R \tag{10a}$$

$$\ddot{r} + 2K_1\dot{r} + K_2 r = \frac{l_F C_F}{I_Z}\dot{\delta}_F + \frac{C_F C_R l}{I_Z m v_x}\delta_F - \frac{l_R C_R}{I_Z}\dot{\delta}_R - \frac{C_F C_R l}{I_Z m v_x}\delta_R \tag{10b}$$

with

$$K_1 = \frac{I_Z(C_R + C_F) + m(C_F l_F^2 + C_R l_R^2)}{2 I_Z m v_x} > 0 \tag{11}$$

$$K_2 = \frac{l^2 C_F C_R + (C_R l_R - C_F l_F) m v_x^2}{I_Z m v_x^2} \gtreqless 0 \tag{12}$$

Here it becomes immediately obvious that the expression

$$(C_R l_R - C_F l_F) m v_x^2 \tag{13}$$

is responsible for the sign of K_2 and the possibility for larger velocities v_x that $K_2 < 0$. This is indicating an unstable steady-state motion of the system. To increase the range of stable behaviour, it will help to put CG closer to the front $l_F < l_R$ and/or 'softer' substitutive tyres at the front $C_F < C_R$ (e.g. applying a stiffer torsion bar at the front axle).

2.2 Steady State Cornering Without Rear Wheel Steering ($\delta_R = 0$)

In general the common passenger car layout does not have additional rear wheel steering, but this feature may be used for control purposes in the near future. An essential information regarding the vehicle behaviour with respect to the influence of the cornering radius and the velocity is provided by the steady state condition,

where the cornering radius is equal to the curvature radius $\rho = R$ and

$$v = \text{const.} \tag{14}$$

$$\dot{\psi} = r = v/R \tag{15}$$

$$a_y = v^2/R \tag{16}$$

The steady state values for the steering angle and the side slip angle of the car derive directly from (10a) and (10b) with (14) and with $\delta_R = 0$:

$$\delta_{F,st} = \delta_{Fo} + \frac{C_R l_R - C_F l_F}{C_R C_F l} m a_{y,st} \tag{17}$$

$$\beta_{st} = \beta_o - \frac{l_F}{C_R l} m a_{y,st} \tag{18}$$

Using the condition $v \to 0$ the corresponding values of side slip angle and steering angle (also denoted Ackermann angle δ_a) are, see Fig. 2:

$$\beta_o = \frac{l_R}{R}, \quad \delta_a = \delta_{Fo} = \frac{l}{R} = \frac{l}{v_x^2} a_{y,st}, \quad \beta_o = \frac{l_R}{l} \delta_{Fo} \tag{19}$$

To characterize the steering behaviour, an understeer gradient is used:

$$K_{US} = \frac{m(C_R l_R - C_F l_F)}{C_R C_F l} \gtrless 0 \tag{20}$$

Consequently (17) can be modified, and with the sign of K_{US} the increase/decrease of the necessary steering angle with increasing values of velocity or acceleration can be explained.

$$\frac{\delta_{H,st}}{i_s} = \delta_{F,st} = \delta_{F0} + K_{US} a_{y,st} \tag{21}$$

As indicated in (21) also the hand wheel steering angle $\delta_{H,st}$ together with the steering system ratio i_s is introduced. Thus, (21) and K_{US} may be used to characterise the steering behaviour of the vehicle:

$K_{US} >$ understeer behaviour
$K_{US} =$ neutral steering
$K_{US} <$ oversteer behaviour

For a graphical presentation of a typical behaviour two kinds of figures are common. With the data given in Table 1 for an oversteer vehicle A and an understeer vehicle B the Fig. 3 shows the change of steering angle δ_F for constant velocity as function of

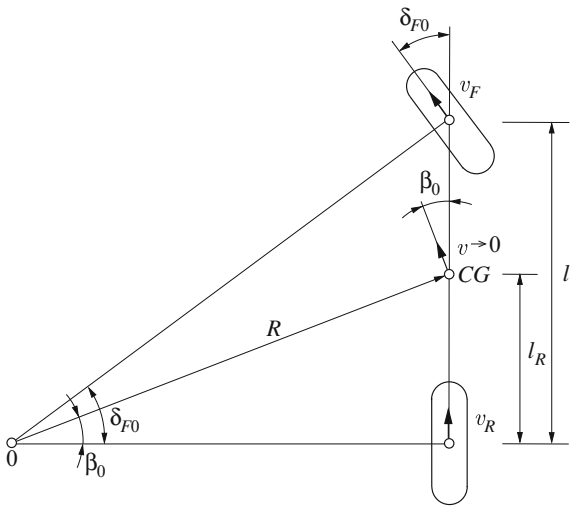

Fig. 2 Driving condition for $v \to 0$

Table 1 Vehicle data for the linear 2-wheel models used for the demonstration examples: two different steering characteristics

Vehicle	**A**	**B**
m	1900 kg	
I_Z	2900 kgm²	
l_F	1.44 m	
l_R	1.36 m	
C_F	90 000 N rad^{-1}	60 000 N rad^{-1}
C_R	80 000 N rad^{-1}	110 000 N rad^{-1}
K_{US}	$-1.95 \cdot 10^{-3}$ s² m^{-1}	$+6.50 \cdot 10^{-3}$ s² m^{-1}
Steering characteristics	oversteer	understeer

lateral acceleration a_y (for variation of R) and constant radius R as function of lateral acceleration a_y (for variation of v), Lugner (2007).

For the oversteer vehicle A with increasing a_y the necessary steering angle δ_F decreases. Consequently an increasing sensitivity of the driver is necessary for proper steering. The understeer vehicle B needs increasing steering angles δ_F with increasing a_y, a property that for the driver fits to the expected behaviour. Though the steering behaviour is quite different for vehicles A and B, the side slip angle β characteristics do not show greater differences with increasing a_y. For both vehicles the $\beta < 0$ indicates an inward turned attitude during cornering.

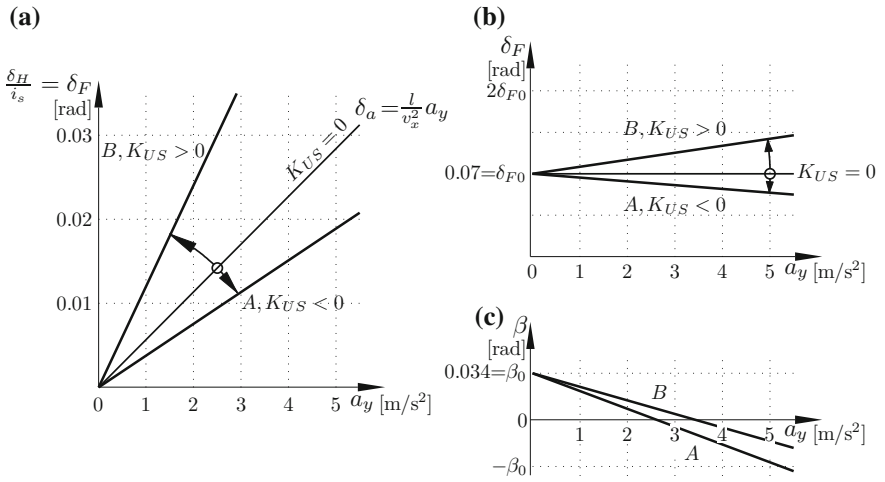

Fig. 3 Steady state steering characteristics, data corresponding to Table 1: **a** for $v = \text{constant} = 80$ km/h; **b** for $R = \text{constant} = 40$ m; **c** side slip angles to (**b**)

2.3 Steady State Cornering with Rear Wheel Steering $\delta_R \neq 0$

The effects of additional rear wheel steering, representing an additional system input, make it possible to change/improve the steering behaviour or the side slip angle of the car.

For cornering with very low speed ($v \to 0$), Fig. 4 provides

$$\frac{l}{R} = \delta_{Fo} - \delta_{Ro} \tag{22}$$

$$\beta_{Ro} = \frac{l_R}{l}\delta_{Fo} + \frac{l_F}{l}\delta_{Ro} = \frac{l_R}{R} + \delta_{Ro} \tag{23}$$

according to the relation of these two steering inputs. So δ_{Ro} may be chosen in such a way that $\beta_{Ro} = 0$ for left/right cornering.

For velocities or accelerations larger than zero the equation corresponding to (17) becomes

$$\delta_{F,st} - \delta_{R,st} = \delta_{Fo} - \delta_{R_o} + \frac{C_R l_R - C_F l_F}{C_F C_R l} m a_{y,st} \tag{24}$$

It is obvious that for constant $\delta_{Fo} - \delta_{Ro}$ and no further change of the rear wheel steering angle (e.g. $\delta_{R,st} = 0$), the characterisation for under-, neutral- and oversteer behaviour is the same as before. On the other hand, if $(\delta_{R,st} - \delta_{Ro})$ is used as a variable input—e.g. by a control system—one may achieve an arbitrary steering behaviour.

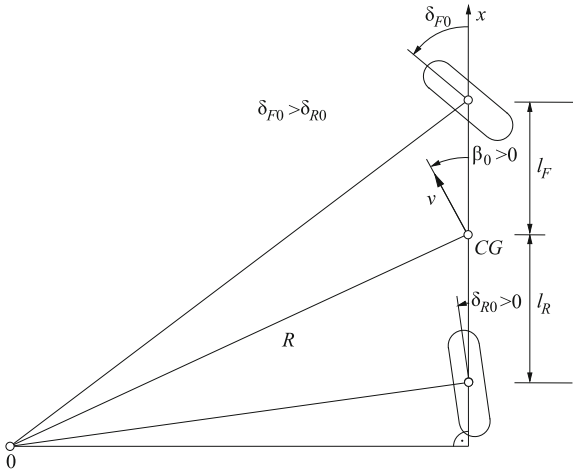

Fig. 4 Additional rear wheel steering: steady state cornering with $v \to 0$

Assuming that there is no change of the initial rear wheel steering angle δ_{R0}, and $\delta_{R,st} = 0$, the side slip angle of the vehicle will become

$$\beta_{R,st} = \beta_{Ro} + (\delta_{R,st} - \delta_{Ro}) - \frac{l_F}{C_R l} m a_{y,st} \tag{25}$$

Compared to (19), this relation indicates a shift in β_{st} only.

In contrast to (10a) it can be shown that, with a proper control, the side slip angle β of the car can be hold at $\beta_{st} = 0$—as considered to be desirable in literature.

$$\beta_{st} = 0 = \delta_F \left(\frac{l_R}{l} - \frac{C_F l_F m v_x^2}{l^2 C_F C_R} \right) + \delta_R \left(\frac{l_F}{l} + \frac{C_R l_R m v_x^2}{l^2 C_F C_R} \right) \tag{26}$$

Especially in tight curves with $v_x \to 0$ this control aim may help the driver regarding the orientation of the vehicle motion and the direction of his/her view. If it is wanted to have both a given steering (wheel) characteristic for the driver and the side slip angle $\beta = 0$, an additional front wheel steering $\Delta\delta_F$ or a variable steering ratio i_s need to be used.

2.4 Stability

Under certain conditions the motion of the car—represented by the linear differential equations (9) or (10)—can become unstable. Even small disturbances at steady state driving conditions will result in uncontrolled motions, e.g. Mitschke and Wallentowitz (2014), Rill (2012).

The eigenvalues of the equations of motion characterize the stability behaviour. As well known, the eigenvalues $\lambda_{1,2}$ can be derived from the homogenous part of the differential equations (9) or (10) by

$$\det(\mathbf{F} - \lambda\mathbf{E}) = 0 \tag{27}$$

(where $\mathbf{E}$ represents the unity matrix) or

$$\lambda^2 + 2K_1\lambda + K_2 = 0 \tag{28}$$

From (28) the eigenvalues follow immediately with

$$\lambda_{1,2} = -K_1 \pm \sqrt{{K_1}^2 - K_2} \tag{29}$$

In general, stability is given as long as the real parts of the eigenvalues are smaller than zero. The system will show an unstable behaviour if $K_2 < 0$. To determine the sign of K_2 Eq. (12) leads to

$$\begin{aligned} l^2 C_F C_R + (C_R l_R - C_F l_F) m {v_x}^2 &\gtreqless 0 \\ l + \frac{(C_R l_R - C_F l_F)}{l C_R C_F} m {v_x}^2 &\gtreqless 0 \end{aligned} \tag{30}$$

So it is immediately obvious that the expression (see (13))

$$(C_R l_R - C_F l_F) m v_x^2 \tag{31}$$

is responsible for the sign of K_2 and the possibility for larger velocities v_x that $K_2 < 0$ indicates the instability of the system.

Using (20) Eq. (30) can be expressed by

$$\delta_{F0} + K_{US} a_{y,st} \gtreqless 0; \tag{32}$$

which is identical with the right hand side of (21). So the sign of the understeer gradient K_{US} is also informative regarding the stability. An oversteer vehicle can become unstable for higher velocities/accelerations.

Since only the homogenous equations are employed for the determination of the stability, the criterion (32) for a car with additional rear wheel steering needs to be modified due to (24) to

$$\delta_{F0} - \delta_{R0} + K_{US} a_{y,st} \gtreqless 0 \tag{33}$$

Since $\delta_{R0} \gtreqless 0$ the lateral acceleration $a_{y,st}$ for the stability limit can be changed compared to pure front wheel steering.

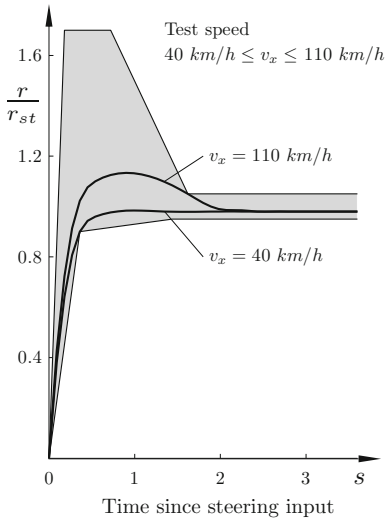

Fig. 5 Steering step input limits defined by *ESV* (Experimental Safety Vehicle): with two examples of a passenger car (step input $\dot{\delta}_H \cong 500°/\text{s}$, final steady state lateral acceleration $a_{y,st} \cong 0.4g$)

2.5 Step Steering Input

In critical situations it may happen that the driver will introduce a step like steering input. Then the response of the vehicle can be characterized e.g. by the yaw velocity r which will reach the steady state value r_{st} after the transient phase following the input. Figure 5 shows accepted limits for $r(t)$.

The corresponding steady state straight ahead driving yaw velocity gain (see (10b)) is defined by

$$G_{r,st} = \frac{r}{\delta_H / i_s}\Big/_{st} = \frac{v_x}{l + K_{US} {v_x}^2} \tag{34}$$

where the denominator is already introduced with (30).

For an understeer vehicle $K_{US} > 0$ the gain $G_{r,st}$ will have a maximum at a characteristic speed v_{ch} that can be obtained by

$$\frac{\partial G_{r,st}}{\partial v_x} = \frac{l - K_{US} v_{ch}^2}{(l + K_{US} v_{ch}^2)^2} = 0$$

$$v_{ch}^2 = \frac{l}{K_{US}}, \quad K_{US} > 0 \tag{35}$$

In contrast, the oversteer vehicle $K_{US} < 0$ will have an unlimited yaw response for the critical speed v_{crit}

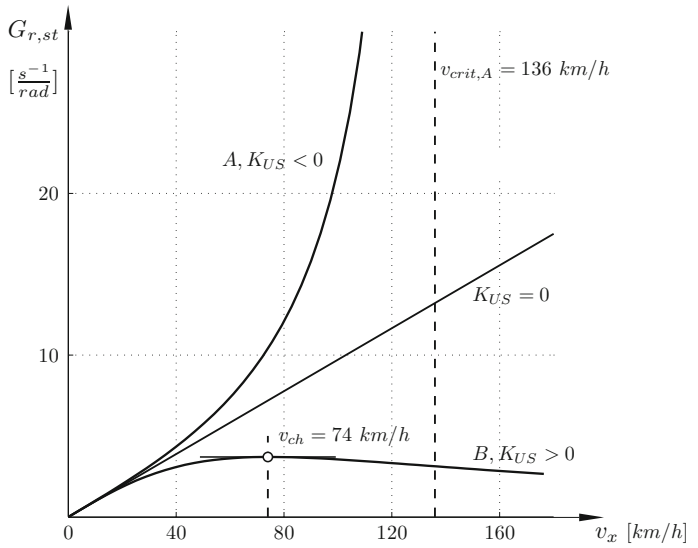

Fig. 6 Behaviour of oversteer, neutral and understeer vehicle with respect to the static yaw velocity gain; vehicle data for A, B according Table 1

$$G_{r,s} \Rightarrow \infty$$
$$v_{crit}^2 = -\frac{l}{K_{US}}, \quad K_{US} < 0 \tag{36}$$

Figure 6 shows for the already introduced vehicles A and B (see Table 1) the yaw velocity gains. The understeer vehicle B shows a nearly equal response for 40 km/h and more—a driver friendly behaviour. The increasing response of vehicle A will be a challenge for the driver even for velocities smaller than the critical one.

The corresponding acceleration response is shown in Fig. 7. With the steady state acceleration

$$a_{y,st} = r\, v_x$$

the lateral acceleration response

$$\frac{a_y}{\delta_H / is}\Big/_{st} = G_{ay,st} = \frac{v_x^2}{l + K_{US} {v_x}^2} \tag{37}$$

has the same structure as the yaw response. The understeer vehicle B has a limitation for the $a_{y,st}$ while even a neutral steering vehicle tends to have nonlinear increasing values of $G_{ay,st}$.

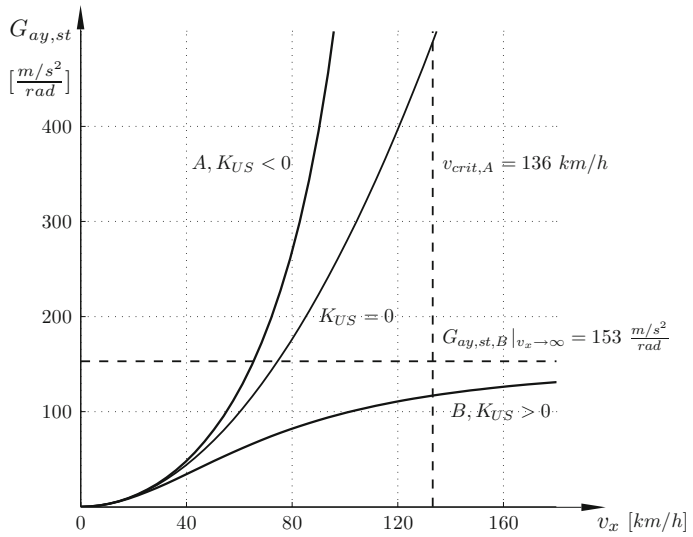

Fig. 7 Steady state lateral acceleration gain for oversteer $K_{US} < 0$, neutral steer $K_{US} = 0$ and understeer vehicle $K_{US} > 0$; vehicle data for A, B according to Table 1

2.6 Frequency Response

To provide an information for an alternating steering the vehicle reaction to harmonic inputs of different frequencies can be considered. It is assumed that the driver starts the harmonic input at straight ahead driving; no rear wheel steering is taken into account.

The yaw velocity frequency response for frequency ν results again from Eq. (10):

$$G_r(i\nu) = (\frac{r}{\delta_F})|_{i\nu} = G_{r,st}\frac{1 + T_Z(i\nu)}{1 + \frac{2D}{\omega_o}(i\nu) - \frac{\nu^2}{\omega_o^2}} \tag{38}$$

with

$$T_Z = \frac{m v_x l_F}{C_R l}$$

$$\omega_o^2 = K_2 = \frac{C_F C_R l^2}{I_Z m v_x^2}(1 + \frac{K_{US} v_x^2}{l})$$

$$D\omega_o = K_1$$

The response for the lateral acceleration can be calculated using also (10) and

$$a_y = v_x(r + \dot{\beta})$$

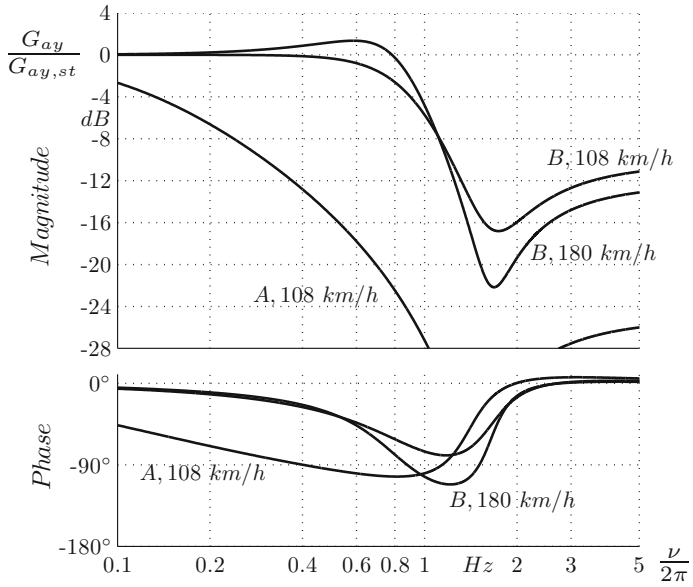

Fig. 8 Normalized acceleration frequency response of the oversteer vehicle A and the understeer vehicle B (Table 1). No response of vehicle A for $v > v_{crit} = 136$ km/h

$$\frac{a_y(i\nu)}{\delta_F(i\nu)} = v_x[\frac{r(i\nu) + i\nu\beta(i\nu)}{\delta_F(i\nu)}]$$

$$G_{ay}(i\nu) = (\frac{a_y}{\delta_F}) = G_{ay,st}\frac{1 + T_1(i\nu) - T_2\nu^2}{1 + \frac{2D}{\omega_o}(i\nu) - \frac{\nu^2}{\omega_o^2}} \tag{39}$$

with

$$T_1 = \frac{l_R}{v_x} \quad , \quad T_2 = \frac{I_z}{C_R l}$$

and D, ω_0 corresponding to (38).

With Fig. 8 it can be noticed that for the lateral acceleration gain in the region of normal steering till about 1 Hz the oversteer vehicle shows a strongly frequency dependent response with large phase angles compared to the driver friendly behaviour of vehicle B. The low steering response behaviour about 1–2 Hz is a generally accepted feature.

Examples for measured frequency responses are shown in Fig. 9 for an understeer vehicle.

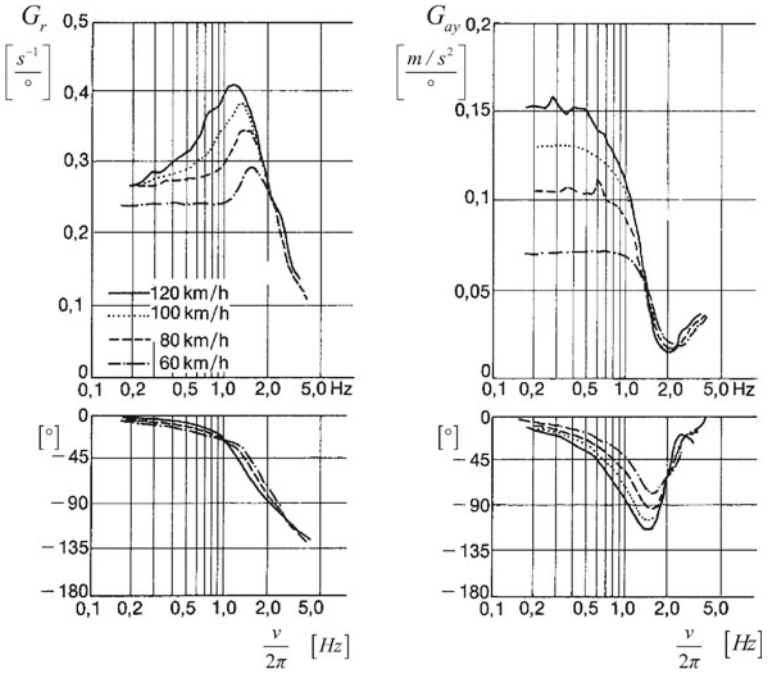

Fig. 9 Measurements of yaw velocity and lateral acceleration responses of an understeer vehicle ($K_{US} = 0.0062\ s^2m^{-1}$, $v_{ch} = 76$ km/h) similar to vehicle A for different driving velocities, Lugner (2007)

2.7 Longitudinal Dynamics, x-z-plane

To investigate the influences of braking or accelerating a plane vehicle model like Fig. 10 is introduced, Plöchl et al. (2015), Lugner (2007). Thereby no heave and pitch motions are taken into account.

If the individual rotations of the wheels are included further extensions with respect to the configuration of the drive train (four-wheel drive, electric hub drive,

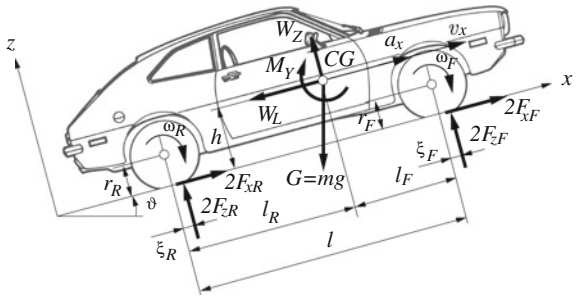

Fig. 10 Plane vehicle model for longitudinal dynamics; symmetry to central *x*-*z*-plane

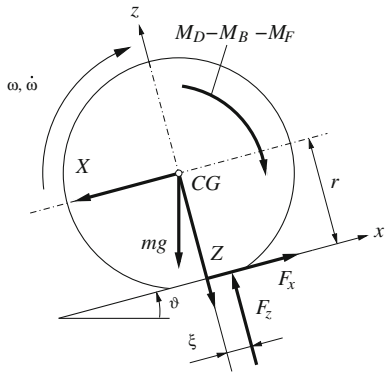

Fig. 11 Model of a wheel

etc.) and at least the sticking and slipping of a wheel can be considered. Correspondingly Fig. 11 shows the essential features of the wheel motion. It is assumed that in the wheel hub—also the *CG* of the wheel—the forces X, Z are transferred to the axle. The normal force F_z has an offset, the pneumatic trail ξ, which represents the rolling resistance. M_D, M_B, M_F, are driving torque, braking torque and friction moment by the wheel bearing.

For the kinematics, the simplification that the tyre radius r is equal to the rolling radius is assumed.

The equations of motion for the vehicle Fig. 10 now can be established:

$$ma_x = 2F_{xF} + 2F_{xR} - W_L - G\sin\vartheta \tag{40}$$

$$0 = 2F_{zF} + 2F_{zR} + W_Z - G\cos\vartheta \tag{41}$$

$$2I_F\dot{\omega}_F + 2I_R\dot{\omega}_R = 2F_{zR}(l_R - \xi_R) - 2F_{zF}(l_F + \xi_F) - 2(F_{xF} + F_{xR})h + M_Y \tag{42}$$

With the aerodynamic components W_L, W_Z, M_Y, the moments of inertia I_F, I_R of the wheels with respect to their axes and the whole vehicle mass m. The angular acceleration of e.g. the rear wheel can be calculated by

$$I_R\dot{\omega}_R = M_{DR} - M_{BR} - M_{FR} - F_{zR}\xi_R - F_{xR}r_R \tag{43}$$

with the drive torque M_{DR}, the braking moment M_{BR} and possible small friction effects with $M_{FR} \approx 0$.

To determine the effects of the drive train configuration by Eqs. (40)–(43), the longitudinal acceleration a_x initiated by the drive/brake forces has to be considered. Assuming pure rolling of the wheels and

$$\begin{aligned} r_R\omega_R = r_F\omega_F = r\omega = v_x \\ r\dot{\omega} = a_x \end{aligned} \tag{44}$$

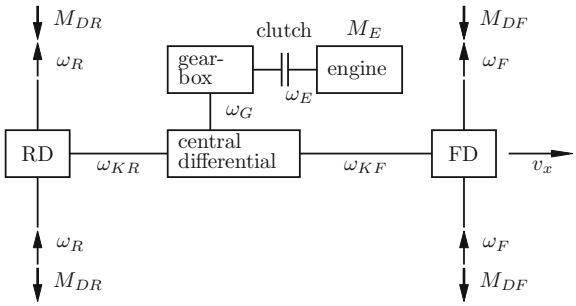

Fig. 12 Structure of a drive train with axle and central differentials

the longitudinal acceleration of the vehicle becomes

$$(m + \frac{2I_R}{r^2} + \frac{2I_F}{r^2})a_x = \frac{M_D}{r} - \frac{M_B}{r} - W_{ges} \tag{45}$$

with the substitutes

$$\begin{aligned} W_{ges} &= \frac{M_F}{r} + W_R + W_L + W_G \\ \xi_F/r &= \xi_R/r = f_R \\ W_R &= f_R(2F_{zR} + 2F_{zF}) = f_R(G\cos\vartheta - W_Z) \\ W_G &= mg\sin\vartheta \\ M_F &= 2(M_{FR} + M_{FF}) \approx 0 \\ M_D &= 2M_{DR} + 2M_{DF} \\ M_B &= 2M_{BR} + 2M_{BF} \end{aligned}$$

A drive train configuration with symmetric structure, angular velocity ω_E of the engine and ω_{KR}, ω_{KF} for the front and rear drive shafts is established with Fig. 12.

With the transmission ratio N_{Gn} of the gear box and the ratio N_D of the axle differentials and the torque splitting of the central differential with ν_F, ν_R, the kinematics become

$$\begin{aligned} \omega_E &= \omega_G N_{Gn}, \\ \omega_G &= \nu_R\omega_{KR} + \nu_F\omega_{KF} \\ \omega_{KR} &= N_D\omega_R, \quad \omega_{KF} = N_D\omega_F \end{aligned} \tag{46}$$

and the torques for the different kind of drives

$$
\begin{aligned}
2M_{DF} = M_D \nu_F, \quad 2M_{DR} &= M_D \nu_R \\
\text{with } \nu_F + \nu_R &= 1 \\
\text{for rear wheel drive}: \quad \nu_R &= 1 \\
\text{for front wheel drive}: \quad \nu_F &= 1 \\
\text{for 4WD with equal distribution}: \quad \nu_R &= \nu_F = 0.5
\end{aligned} \tag{47}
$$

The torque transfer from the engine torque $M_E(\omega_E)$ to the wheels, using (44), can be written by

$$M_D = (2M_{DF} + 2M_{DR}) =$$

$$\eta M_E(\omega_E) N - r\left[\frac{\Theta_E N^2}{r^2} + \frac{(I_C + I_{DR} + I_{DF})}{r^2} N_{Gn}^2\right] a_x \tag{48}$$

with

$$N = N_{Gn} N_D$$

η coefficient of efficiency
Θ_E substitutive moment of inertia for the engine
I_C moment of inertia for parts of gears and central differential
I_{DF}, I_{DR} moments of inertia: parts of differentials and shafts.

Consequently (45) can be transformed to

$$(m + m_r) a_x = \frac{\eta M_E \omega_E N}{r} - \frac{M_B}{r} - W_{ges} \tag{49}$$

with the reduced mass for the rotational parts:

$$m_r = \frac{1}{r^2}\left[\Theta_E N^2 + (I_C + I_{RD} + I_{FD}) N_{GN}^2 + (2I_R + 2I_F)\right]$$

To determine the normal forces F_{zi} and further on the friction limits for the force transfer of the tyres, again Eqs. (41) and (42) are used. With the simplification of pure rolling (44) and equal values $\xi_R = \xi_F = \xi$, these equations can be written in the form

$$
\begin{aligned}
2F_{zF} + 2F_{zR} &= G\cos\vartheta - W_z \\
-2l_F F_{zF} + 2l_R F_{zR} &= \left[\left(\frac{2I_F}{r} + \frac{2I_R}{r}\right) a_x + (m a_x + W_L + G\sin\vartheta) h \right. \\
&\quad \left. + M_Y + \xi(G\cos\vartheta - W_Z)\right]
\end{aligned} \tag{50}
$$

Linearization and neglecting small terms and aerodynamic components leads to

$$M_Y \cong 0, \quad W_Z \cong 0$$
$$\xi(G\cos\vartheta) \ll (ma_x + W_L + G\sin\vartheta)h$$
$$(2I_F + 2I_R)/r \ll mh$$

$$\frac{F_{zF}}{G} = \frac{l_R}{l}\cos\vartheta - a^*\frac{h}{l} \qquad (51)$$
$$\frac{F_{zR}}{G} = \frac{l_F}{l}\cos\vartheta + a^*\frac{h}{l}$$

$$\text{with} \quad a^* = \left(\frac{a_x}{g} + \sin\vartheta + \frac{W_L}{mg}\right) \qquad (52)$$
$$q = 100 \cdot \tan\vartheta \ \text{ in\%}$$

If the inclination angle ϑ is small (road grade q less than about 10%), then the sin-function can be linearized too.

With the determination of the normal forces, the rolling resistance W_R, see (45), can be calculated. Corresponding to Fig. 11 without M_D, M_B, M_F and no grade $\vartheta = 0$, the longitudinal force due to tyre flexibility and energy dissipation can be written with

$$F_x = -\frac{\xi}{r}F_z = -f_R F_z \qquad (53)$$

Some examples for typical values of the rolling resistance coefficient f_R are shown in Fig. 13, see e.g. Plöchl et al. (2014). As expected the energy dissipation increases at higher speeds, but in the limits by traffic regulations it is nearly constant.

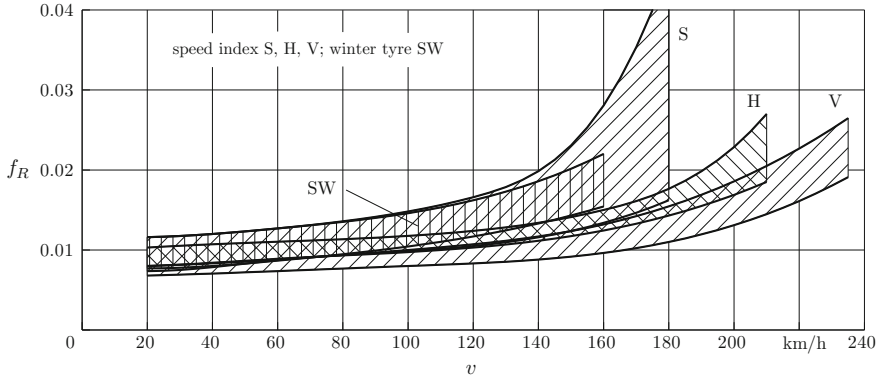

Fig. 13 Rolling resistance coefficient f_R for different types of passenger car tyres

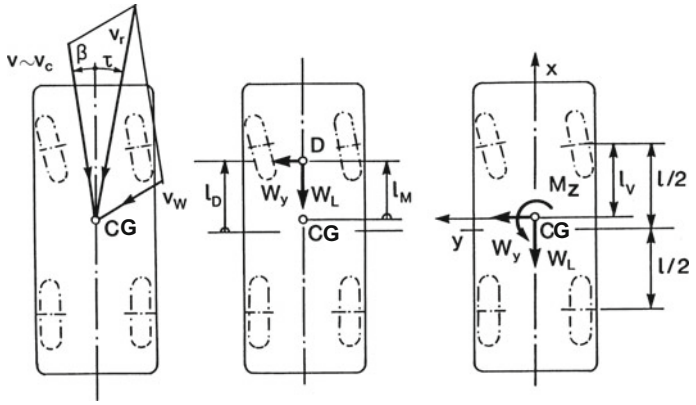

Fig. 14 Aerodynamic forces W_y, W_L and moment M_Z by running speed v_c and ambient wind v_W; plane motion

The consequences of the aerodynamics for a vehicle running with v and ambient wind v_W, are shown in Fig. 14, Mitschke and Wallentowitz (2014), Kortüm and Lugner (1994).

With the cross section area A and aerodynamic coefficients c_i, the forces are presented by

$$\begin{aligned} W_L = W_X &= c_x(\tau) A \cdot \frac{{v_r}^2 \rho}{2} \\ W_Y &= c_y(\tau) A \cdot \frac{{v_r}^2 \rho}{2} \\ M_Z &= c_M(\tau) l_M A \cdot \frac{{v_r}^2 \rho}{2} \end{aligned} \tag{54}$$

The coefficients are determined by experiments in a wind tunnel or/and also by software packages calculating the aerodynamic flow.

To take into account the angle of attack τ, the coefficients are considered to be functions of τ. Defining the coefficient for calm air with $c_w = c_x(\tau = 0)$ as an example, Fig. 15 shows the normalized value $c_x(\tau)/c_w$, Kortüm and Lugner (1994). The values of the coefficient vary depending on the shape of the car body and will be about $c_w \sim 0.3$ for passenger cars. The position for point D can be estimated with $l_D \cong 0.3l$ for passenger cars and $l_D \cong 0.17l$ for more squared like shapes.

To provide driving performance information with respect to available engine torque M_E, transferred to the wheels or corresponding longitudinal forces, the engine characteristics and drive train structure have to be known.

Figure 16 shows the typical maximal driving torque $M_{E,max}(n_E)$ and power $P_{max}(n_E)$ of a gasoline engine as function of the engine speed $n_E = 60(\omega_E/2\pi)$ for steady state conditions, Lugner (2007).

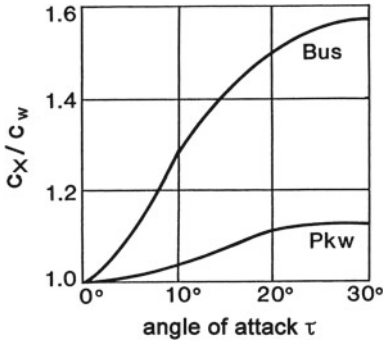

Fig. 15 Normalized drag coefficient $c_x(\tau)/c_w$ as function of the angle of attack τ

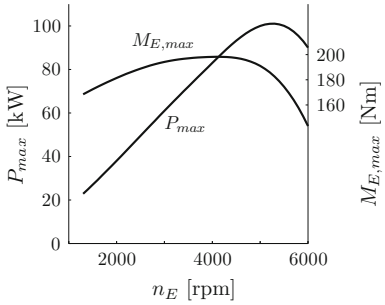

Fig. 16 Maximum torque $M_{E,max}$ and power P_{max} of a gasoline combustion engine

Considering the influence of the throttle position λ_T and the engine drag $M_{E,d}(n_E)$ an approximation for the available engine torque can be formulated. For low velocities/engine speeds, due to the fuel injection, at $\lambda_T = 0$ the drag $M_{E,d}(n_E) > 0$. In the range of operation, $M_{E,d}$ is approximated by a linear function of n_E.

$$M_E = (M_{E,max} - M_{E,d}) f(\lambda_T) + M_{E,d}, \quad 0 \le f(\lambda_T) \le 1 \tag{55}$$

So with the knowledge of $f(\lambda_T)$ and the characteristics for $M_{E,max}$ and $M_{E,d}$ the whole performance volume of the engine can be presented. Furthermore the transmission ratio N can be introduced. With the effective driving force K_E and W_{ges}—see (49)—the vehicle driving performance becomes

$$\begin{aligned} m\lambda a_x &= K_E(v, N) - W_{ges}(v, N) \\ \lambda &= \frac{m + m_R}{m} \end{aligned} \tag{56}$$

$$K_E = \frac{\eta M_E(n_E) N_D N_{Gn}}{r}, \quad K_{Emax} = \eta \frac{M_{Emax}(n_E)}{r} N_D N_{Gn} \tag{57}$$